REMARKS

Claims 40-60 are pending. Claims 40, 43, 46, 49, 52, and 55 have been amended to even further clarify the claimed subject matter. Claims 40, 46, 52, and 58 are independent.

Page 2 of the Office Action states that the publication by H. Dai et al., entitled "Nanotubes as Nonoprobes in Scanning Probe Microscopy", Nature, Vol. 384, 147-150 (1996), has not been considered even though it was cited in the Information Disclosure Statement filed on March 15, 2004. For the Examiner's convenience, a further copy of that reference is attached hereto. The Examiner is respectfully requested to consider that reference, and confirm for the record in writing that the reference has been considered. It is believed that no fee is required to have the reference considered, because it was cited in the Information Disclosure Statement filed on March 15, 2004. However, if a fee is required, please charge it to Deposit Account 06-1205.

Also, it is respectfully noted that the Examiner did not initial U.S. Application Publication No. 2001-0006232 A1 (*Choi et al.*) listed on page 7/12 of the Form PTO-1449 that was attached to the Information Disclosure Statement filed on March 15, 2004. The Examiner is respectfully requested to acknowledge in writing, for the record, that *Choi et al.* has been considered.

Claims 43, 49 and 55 were objected to for reasons set forth at page 2 of the Office Action. Those claims have been amended to change "distant" to --apart--. Withdrawal of the objection is requested.

Applicant notes the Examiner's comments set forth in the first paragraph appearing at page 3 of the Office Action. It is understood that no response is required to that paragraph at this time. In any event, Applicant does not concede the propriety of the statements set forth in that paragraph.

Claims 40-60 were rejected under 35 U.S.C. 102(e) as being anticipated by U.S. Patent Application Publication No. 2002/0009637 (*Murakami et al.*).

The filing date of *Murakami et al.* is February 5, 2001, which is later than the September 1, 2000 priority date to which the present application is entitled based on priority Japanese Application No. 2000-265819. A sworn English translation of that priority application was filed on March 15, 2004 in the present application. If the Examiner would like an additional copy, such will gladly be supplied upon request.

In view of the foregoing, it is submitted that *Murakami et al.* does not apply as a reference under Section 102(e) against the presently claimed invention, and thus withdrawal of the Section 102(e) rejection is respectfully requested.

Claims 40-60 have been rejected under 35 U.S.C. 103(a) as being unpatentable over U.S. Patent No. 6,400,091 (*Deguchi et al.*) and the article entitled *Catalytic Engineering of Carbon Nanostructures*, Langmuir 11, pp. 3862-3866 [1995], by Rodriquez et al. (hereinafter "Rodriquez et al.").

According to an aspect of the present invention, a carbon fiber has a structure wherein graphenes are arranged in a particular manner, such as that shown in, for

example, Fig. 12 and described at page 25, lines 4-17 of the specification.[1/] As described at page 26, lines 10-17 of the specification, the electron-emitting device manufactured according to the present invention provides excellent electron emission performance characteristics relative to a carbon nanotube device, such as that shown in, for example, Fig. 11 and described from page 24, line 26 through page 25, line 3, and at page 25, lines 18-23 of the specification.

Owing to each plane of graphenes (forming a path along which an electron moves) being arranged as shown in Fig. 12 according to the invention, so as to extend from a center of the fiber and outwards from sides of the fiber, electrons can be emitted easily from the sides, to provide excellent electron emission performance. See, e.g., from page 26, line 10 through page 27, line 10 of the specification, for a description relating to electron emission characteristics achieved by the present invention.

In the carbon nanotube shown in Fig. 11, on the other hand, which is similar to *Deguchi et al.*, a direction of graphene orientation is in parallel to the fiber axis. Accordingly, electrons move substantially along the fiber axis, and can be emitted only from the fiber end.

The independent claims will now addressed.

Independent Claim 40 recites a method of manufacturing an electron-emitting device having a plurality of carbon fibers and first and second electrodes disposed

---

1/ Of course, any embodiments referred to herein are mentioned for purposes of illustration only, and the scope of the claimed invention should not be construed as being limited only thereto.

on a substrate. The method comprises the steps of providing the substrate on which the first electrode and the second electrode are disposed, and arranging the plurality of carbon fibers on the first electrode. Each carbon fiber has a plurality of graphenes stacked in a direction different from a direction perpendicular with respect to an axis direction of each carbon fiber.

Independent Claim 46 recites a method of manufacturing an electron-emitting device having a plurality of carbon fibers and first and second electrodes disposed on a substrate. The method comprises the steps of providing the substrate on which the first electrode and the second electrode are disposed, and arranging the plurality of carbon fibers on the first electrode. Each carbon fiber comprises a plurality of stacked graphenes intersecting with an axis of the carbon fiber.

Independent Claim 52 is directed to a method of manufacturing an electron-emitting device having a plurality of carbon fibers and first and second electrodes disposed on a substrate. The method comprises the steps of providing the substrate on which the first electrode and the second electrode are disposed, and arranging the plurality of carbon fibers on the first electrode. Each carbon fiber has a plurality of graphenes, and the graphenes are stacked along an axis direction of the carbon fiber.

Independent Claim 58 is directed to a method of manufacturing an electron-emitting device, comprising the steps of providing a first electrode disposed on a substrate,

arranging a second electrode on the substrate, and arranging a plurality of carbon fibers on the first electrode. Each carbon fiber comprises a plurality of graphenes which are stacked so as not to be parallel to an axis direction of the fiber.

The Office Action concedes that *Deguchi et al.* does not teach or suggest the features of the independent claims relating to the manner in which graphenes are stacked, but then asserts that *Rodriquez et al.* teaches these features, and also that it would have been obvious to one of ordinary skill in the art to modify the carbon fibers of *Deguchi et al.* based on *Rodriquez et al.* to provide the graphene structures recited in the independent claims. However, the rejection is respectfully traversed for the following reasons.

First, *Deguchi et al.* discloses diamond, graphite and carbon nanotube as a carbon allotrope which may be suitably used in the electron emission member. However, the *Deguchi et al.* device is similar to that referred to above and shown in Fig. 11 of the present application. Nothing in *Deguchi et al.* would disclose or suggest a carbon fiber of a crystal structure, such as that recited in the independent claims, let alone a configuration other than a carbon nanotube as described in *Deguchi et al.* , for use in an electron-emission member.

Second, *Rodriguez et al.* neither discloses nor suggests providing a carbon nanofiber in an electron-emitting device, let alone a need to improve electron emitting characteristics of an electron-emitting device.

Accordingly, there would have been no reason why one skilled in the relevant art who was faced with the same problem of improving electron emission

characteristics, as was confronted by Applicant at the time of his invention, would have even consulted *Rodriquez et al.*, let alone been motivated to attempt to combine it with *Deguchi et al.*, as proposed in the Office Action. Indeed, the Office Action's suggestion to combine *Deguchi et al.* and *Rodriquez et al.* seemingly relies on impermissible hindsight reasoning, since it proposes to combine the references to achieve a result gleaned solely from Applicant's disclosure, without any teaching, suggestion, or motivation in the prior art to do so. Uniroyal, Inc. v. Rudkin-Wiley Corp., 837 F.2d 1044, 1051-52, 5 USPQ 2d 1434, 1438 (Fed. Cir. 1988) (it is impermissible to reconstruct the claimed invention from selected pieces of prior art absent some suggestion, teaching, or motivation in the prior art to do so); In re Fritch, 972 F.2d 1260, 23 USPQ 2d 1780 (Fed. Cir. 1992) ("[I]t is impermissible to use the claimed invention as an instruction manual or 'template' to piece together the teachings of the prior art so that the claimed invention is rendered obvious. . . . This court has previously stated that '[o]ne cannot use hindsight reconstruction to pick and choose among isolated disclosures in the prior art to deprecate the claimed invention.'").

It is respectfully submitted that neither *Deguchi et al.* nor *Rodriquez et al.* discloses or suggests a method for manufacturing an electron-emitting device wherein graphenes are stacked in the manner set forth in the independent claims, and thus those claims are believed to be clearly patentable over those references, whether considered separately or in combination.

For all of the foregoing reasons, Applicant respectfully submits that the Examiner has failed to establish a prima facie case of obviousness against the independent claims herein, and thus withdrawal of the Section 103(a) rejection is respectfully requested.

The other claims in this application are each dependent from one or another of the independent claims discussed above and are therefore believed patentable over the art relied on in the Office Action for the same reasons as are those independent claims. Since each dependent claim is also deemed to define an additional aspect of the invention, however, the individual reconsideration of the patentability of each on its own merits is respectfully requested.

In view of the foregoing amendments and remarks, Applicant respectfully requests favorable reconsideration and early passage to issue of the present application.

Applicants' undersigned attorney may be reached in our New York office by telephone at (212) 218-2100. All correspondence should continue to be directed to our below listed address.

Respectfully submitted,

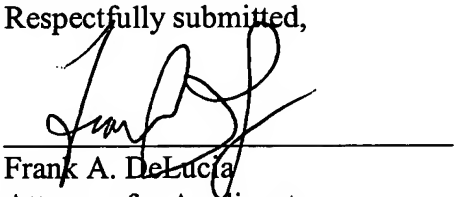

Frank A. DeLucia
Attorney for Applicants
Registration No. 42,476

FITZPATRICK, CELLA, HARPER & SCINTO
30 Rockefeller Plaza
New York, New York 10112-3801
Facsimile: (212) 218-2200

NY_MAIN 536832v1

nature

INTERNATIONAL WEEKLY JOURNAL OF SCIENCE

Volume 384 No. 6605 14 November 1996 $10.00

Revolutionary feeding

Tying the knot by computer

Nanotubes as nanoprobes

The Hedgehog receptor

Neuroscience

free to oscillate in air. We have tested the feasibility of this idea by flooding the trenches seen in Fig. 3 with water. Figure 4 shows that the frequency dependence of the cantilever oscillation is only slightly affected when the lower 0.7 μm length of the nanotube is immersed in water within the trench. Also shown in Fig. 4 is the amplitude of the cantilever oscillation as a function of distance from the meniscus at the top of the trench. Note that for the bottom trace which was taken at 235.65 kHz (0.85 kHz above the resonant frequency of the cantilever in air) there is actually an increase in the oscillation amplitude when the MWNT is in the water. We suspect that this effect is due to the elasticity of the meniscus formed around the nanotube at the top of the water layer. Note also that the oscillation amplitude drops sharply when the MWNT tip encounters the SiO_2 surface at the bottom of the trench, permitting SFM imaging of this surface under water at the same frequency and with nearly the same Q obtained in air.

Because the MWNTs are electrically conductive[19,20] they may be used as probes for scanning tunnelling microscopy, STM, and in various scanning electrochemical modes[21,22] as well. Figure 5 shows an example of atomic-scale-resolution STM using a carbon nanotube to image the charge density waves on a freshly cleaved 1T-TaS_2 surface[23].

We have been successful as well in attaching a single 'rope' of single-walled nanotube (SWNT) material[24] to the side of a MWNT probe tip similar to the one shown in Fig. 1. As with the MWNT tip itself, we find it is possible to adjust, at least crudely (±20 nm), the length of the SWNT rope extending out from the tip by applying a voltage pulse that generates a momentary nanoscale arc between the tip and a conductive surface 10–50 nm away. However, to realize the full promise these nanotubes hold as probes of the nanometre world, a more precise method will be needed: one that will guarantee, for example, that just a single (10,10) nanotube[24] extends out the desired length from a bundle of other nanotubes. Laser annealing of the tip of such a single (10,10) tube should ensure that the tip of this SWNT nanoprobe is perfectly closed with a C_{5v} symmetry hemifullerene dome, having a single pentagon centred on the five-fold symmetry axis at the vertex. Used either bare or with chemical derivatization at specific sites on the tip, such a (10,10) tube would be a good candidate for the ultimate nanoprobe. □

Received 7 August; accepted 23 September 1996.

1. Binnig, G. Rohrer, H., Gerber, C. & Weibel, E. *Phys. Rev. Lett.* **50**, 120–123 (1983).
2. Quate, C. F. *Surf. Sci.* **299/300**, 980–995 (1994).
3. Rugar, D. & Hansma, P. *Phys. Today* **43(10)**, 23 (1990).
4. Bustamante, C. & Keller, D. *Phys. Today* **48(12)**, 32–38 (1995).
5. Crommie, M. F., Lutz, C. P. & Eigler, D. M. *Science* **262**, 218–220 (1993).
6. Avouris, P. *Acc. Chem. Res.* **27**, 159–165 (1994).
7. Lieber, C. M., Liu, J. & Sheehan, P. E. *Angew. Chem. Int. Edn Engl.* **35**, 687–704 (1996).
8. Dagata, J. A. *Science* **270**, 1625–1626 (1995).
9. Minne, S. C., Flueckiger, P., Soh, H. T. & Quate, C. F. *J. Vac. Sci. Technol. B* **13(3)**, 1380–1384 (1995).
10. Shen, T.-C. *et al. Science* **268**, 1590–1592 (1995).
11. Iijima, S. *Nature* **354**, 56–58 (1991).
12. Ebbesen, T. W. *Physics Today* **49(6)**, 26–32 (1996).
13. Colbert, D. T. *et al. Science* **266**, 1218–1222 (1994).
14. Yakobson, B. I., Brabec, C. J. & Bernholc, J. *Phys. Rev. Lett.* **76**, 2511–2514 (1996).
15. Spatz, J. P. *et al. Nanotechnology* **6**, 39–44 (1995).
16. Welsenhorn, A. L., Hansma, P. K., Albrecht, T. R. & Quate, C. F. *Appl. Phys. Lett.* **54**, 2651–2653 (1989).
17. Hansma, H. G., Laney, D. E., Bezanilla, M., Sinsheimer, R. L. & Hansma, P. K. *Biophys. J.* **68**, 1672–1677 (1995).
18. Putman, C. A. J., van der Werf, K. O., de Grooth, B. G., van Hulst, N. F. & Greve, J. *Biophys. J.* **67**, 1749–1753 (1994).
19. Dai, H., Wong, E. E. & Lieber, C. M. *Science* **272**, 523–526 (1996).
20. Ebbesen, T. W. *et al. Nature* **382**, 54–56 (1996).
21. Bard, A. J., Denuault, G., Lee, C., Mandler, D. & Wipf, D. O. *Acc. Chem. Res.* **23**, 357–363 (1990).
22. Husser, O. E., Craston, D. H. & Bard, A. J. *J. Electrochem. Soc.* **136**, 3222–3229 (1989).
23. Dai, H. & Lieber, C. M. *Annu. Rev. Phys. Chem.* **44**, 237–263 (1993).
24. Thess, A. *et al. Science* **273**, 483–487 (1996).
25. Rinzler, A. G. *et al. Science* **269**, 1550–1553 (1995).
26. Treacy, M. M. J., Ebbesen, T. W. & Gibson, J. M. *Nature* **381**, 678–680 (1996).
27. Yakobson, B. I., Brabec, C. J. & Bernholc, J. *Phys. Rev. Lett.* **76**, 2511–2514 (1996).

ACKNOWLEDGEMENTS. We thank R. T. Laaksonen and K. J. Taylor (Texas Instruments) for providing the micro-lithographic trench sample used in the imaging of Fig. 2. This work was supported by the US NSF and the Robert A. Welch Foundation, and the Advanced Technology Program of the State of Texas.

CORRESPONDENCE should be addressed to R.E.S. (e-mail: res@cnst.rice.edu).

Self-replicating amphiphilic monolayers

Rivka Maoz*, Sophie Matlis†, Elaine DiMasi‡, Benjamin M. Ocko‡ & Jacob Sagiv*

* Department of Materials & Interfaces and † Chemical Services Unit, The Weizmann Institute of Science, Rehovot 76100, Israel
‡ Physics Department, Brookhaven National Laboratory, Upton, New York 11973-5000, USA

MOLECULAR films with predetermined layered structures can be engineered by using techniques such as the Langmuir–Blodgett method[1,2] and self-assembly[1,3–9] to deposit discrete monolayers sequentially on a substrate. Such films might have a variety of uses—as smart surface coatings, nonlinear optical materials and in tribology, for example. Here we report the replicative growth of a molecular film of self-assembling silane bilayers with hydrogen-interlayer polar regions into which further identical bilayers can be intercalated. The intercalation step is triggered by a chemical treatment and so can be carried out controllably, allowing duplication in one step of an entire multilayer structure. In this way, we can achieve the stepwise exponential growth of a multilayer film with a predictable number of stacked bilayers.

The quest for artificial molecular entities endowed with the ability to self-replicate in a controllable manner provides much of the stimulus for current research in supramolecular chemistry[10–18]. Particular attention has been given to the study of molecular self-assembly, recognition and organization on a template—elements commonly regarded as prerequisites for the emergence of self-replication in a molecular system. Our recent studies on layer-by-layer self-assembled silane multilayers with interlayer hydrogen bonding[19,20] led us to examine the possibility of using the facile intercalation and template-induced organization in such systems as a means for achieving self-replication.

Here we report on the replicative growth of a solid-immobilized multilayer of oriented long-chain silanes (Fig. 1). We start with an initial hydrogen-bonded bilayer prepared by sequential monolayer self-assembly from solution[20], and proceed through two consecutive steps that involve the acetone-mediated insertion of water into the silane–carboxylic acid interlayer polar space of the pre-assembled bilayer, followed by the spontaneous intercalation of a new silane bilayer (OTS/OTS) into the acetone-treated initial bilayer, upon its immersion in a solution of OTS in bicyclohexyl (BCH; OTS is *n*-octadecyltrichlorosilane.) By repeating this two-step procedure, we observed the repeated deposition of similarly structured OTS/OTS bilayers, the number of fresh bilayers added to the film on completion of each such sequence of operations being equal to the total number of intercalable bilayers already present on the surface. By repeatedly duplicating the entire set of predeposited bilayers, the total number of such bilayers generated on the surface grows as $2^n - 1$, where n is the number of acetone–OTS treatment cycles (Fig. 1).

The stepwise exponential growth of ordered multilayer films, according to the sequence of operations outlined above, is demonstrated by Fourier transform infrared (FTIR) spectra taken before and after each film deposition operation. The FTIR data provide direct evidence for the total amount of film-forming material (OTS) deposited on the surface[19,20], and for the orientation and packing density of the OTS paraffinic tails[20–23] in each deposited layer and the chemical transformations (hydrolysis, condensation) affecting the silane head groups on their incorporation into the growing surface film[20,24,25].

For example, the H–C–H stretch bands (at 2,917 and 2,850 cm^{-1}) of the normalized spectral curves in Fig. 2—representing single NTS and OTS monolayers, the initial bilayer, and thicker films (between 8 and 32 stacked monolayers) produced by the present process—are practically superimposable. (Here NTS

8. Flament, C. *et al. J. Phys. II (France)* **4**, 1021–1032 (1994).
9. Bruinsma, R., Halperin, B. I. & Zippelius, A. *Phys. Rev. B* **25**, 579–582 (1982).
10. Lifschitz, I. M. & Gulida, L. S. *Dokl. Acad. Nauk.* **87**, 377–380 (1952).
11. Peach, M. & Koehler, J. S. *Phys. Rev.* **80**, 436–439 (1950).
12. Pauchard, L. & Meunier, J. *Phys. Rev. Lett.* **70**, 3565–3568 (1993).

ACKNOWLEDGEMENTS. We thank J. Prost, Y. Pomeau and J. Frenken for useful discussions.

CORRESPONDENCE should be addressed to J. M. (e-mail: jmeunier@physique.ens.fr).

Nanotubes as nanoprobes in scanning probe microscopy

Hongjie Dai, Jason H. Hafner, Andrew G. Rinzler, Daniel T. Colbert & Richard E. Smalley

Center for Nanoscale Science and Technology, and Departments of Chemistry and Physics, Rice University, Houston, Texas 77251, USA

Since the invention of the scanning tunnelling microscope[1], the value of establishing a physical connection between the macroscopic world and individual nanometre-scale objects has become increasingly evident, both for probing these objects[2–4] and for direct manipulation[5–7] and fabrication[8–10] at the nanometre scale. While good progress has been made in controlling the position of the macroscopic probe of such devices to sub-ångström accuracy, and in designing sensitive detection schemes, less has been done to improve the probe tip itself[4]. Ideally the tip should be as precisely defined as the object under investigation, and should maintain its integrity after repeated use not only in high vacuum but also in air and water. The best tips currently used for scanning probe microscopy do sometimes achieve sub-nanometre resolution, but they seldom survive a 'tip crash' with the surface, and it is rarely clear what the atomic configuration of the tip is during imaging. Here we show that carbon nanotubes[11,12] might constitute well defined tips for scanning probe microscopy. We have attached individual nanotubes several micrometres in length to the silicon cantilevers of conventional atomic force microscopes. Because of their flexibility, the tips are resistant to damage from tip crashes, while their slenderness permits imaging of sharp recesses in surface topography. We have also been able to exploit the electrical conductivity of nanotubes by using them for scanning tunnelling microscopy.

Multiwalled nanotubes (MWNTs) were prepared in the optimized direct-current carbon arc apparatus reported previously[13]. To use a nanotube as a robust probe we bonded it to the side of the tip of a conventional silicon cantilever using a soft acrylic adhesive 1–10 nm thick (Fig. 1). This permits the nanotube to bend away from its connection whenever the tip is inadvertently 'crashed' into a hard surface, and then to snap back to its original straight position when the tip is withdrawn. Effectively the nanotube is then 'spring loaded' much like the side-view mirror of a car.

When used in tapping-mode scanning force microscopy, SFM (where the change in amplitude of an oscillating cantilever driven near its resonant frequency is monitored as the tip taps the surface; the sharp frequency response of high-quality cantilevers make this technique exquisitely sensitive), a carbon nanotube tip such as that shown in Fig. 1 has the unusual advantage that it is both stiff and gentle. It is stiff because there is no bending of the nanotube at all when it encounters a surface at near-normal incidence until the Euler buckling force[14], F_{EULER} is exceeded:

$$F_{EULER} = \pi^2 YI/L^2 \quad (1)$$

where Y is the Young's modulus, I is the stress moment over the cross-section of the nanotube of radius r ($I \approx \pi r^4/4$) and L is the

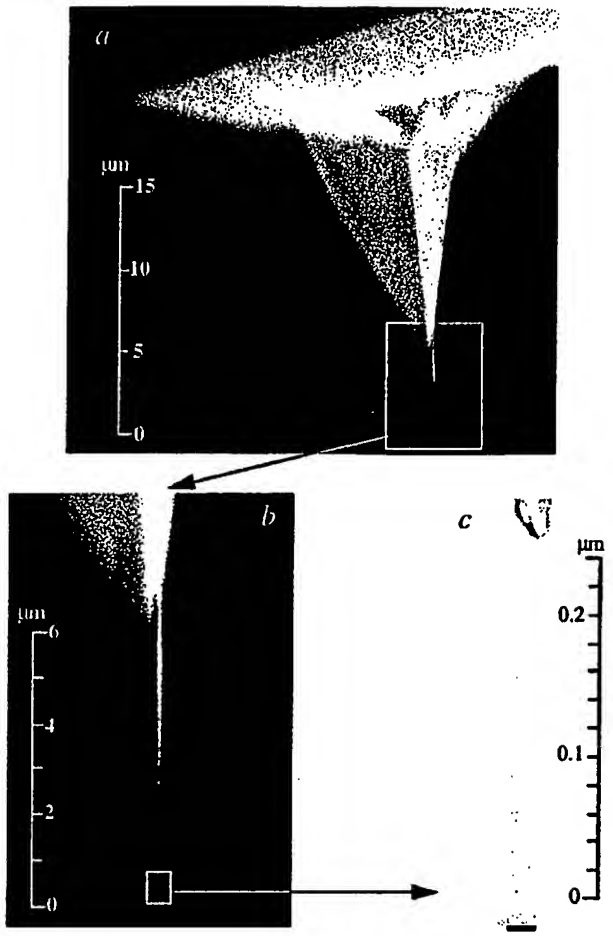

FIG. 1 Single nanotube attached to the pyramidal tip of a silicon cantilever for scanning force microscopy (SFM). The nanotube was attached by first coating the bottom 1–2 μm section of the silicon tip with an acrylic adhesive (by sticking it slightly into an adhesive-coated carbon tape (Electron Microscopy Services, Fort Washington, PA)), and then bringing this tip into contact with the side of a bundle of 5–10 multiwalled carbon nanotubes (MWNTs) while under direct view of an optical microscope using dark-field illumination. Once attached, the nanotube bundle was pulled free from its connections with other nanotubes, leaving a single 5-nm-diameter MWNT extending alone for the final 250 nm. (The most common MWNT diameter obtained at the tip is 5–20 nm, and lengths of single MWNT up to 1 μm are capable of good imaging.) Higher-resolution transmission electron microscopy (TEM) images of this tube showed it to be closed at the tip, as is typical for most MWNTs produced by this arc method (without oxidative etching). *a*, *b*, Scanning electron microscope (SEM) images showing the MWNT bundle attached to the steeper slope of the back side of the silicon pyramid. This attachment ensured that the individual MWNT extending out the end of the bundle, as seen in the TEM image *c*, would approach the surface to be imaged within a few degrees of vertical. Although the adhesive bonding is restricted to within 1–2 μm of the apex, the MWNT bundle continues 5–10 μm further along the side of the pyramid in van der Waals contact. If the pyramid itself is pre-coated with a layer of conductive metal, this method produces a good electrical contact to the MWNT bundle and thereby to the single MWNT probe tip at the end[25]. This attachment method is simple and reliable once the requisite microscope and micro-manipulators are set up. With good-quality MWNT material, mounted probes similar to that shown can be obtained after a few tries. It is useful to have ready access to an electron microscope with a specially-adapted specimen holder to view the cantilever after the MWNT bundle has been attached to see whether the final MWNT at the tip is of the length and diameter desired; after some experience, however, one can simply try imaging with the tips and electro-shortening if necessary. Scale bar in *c*, 20 nm.

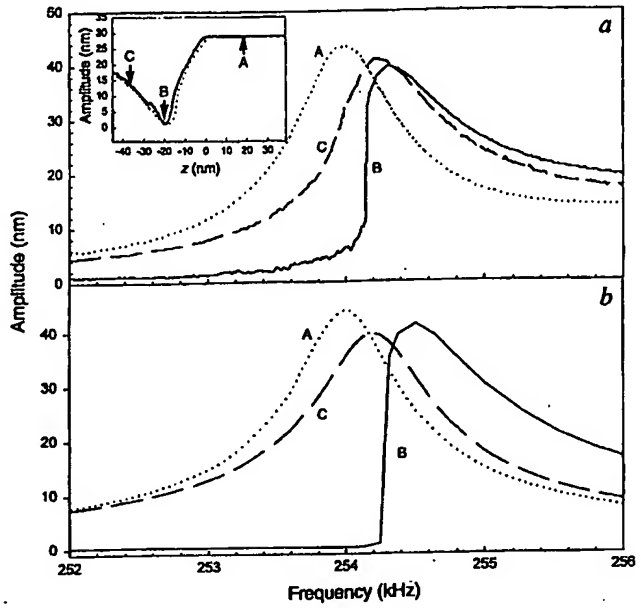

FIG. 2 Frequency response of cantilevers with mounted nanotube tips. The inset of panel *a* shows the tapping amplitude change as a function of distance (z) between a freshly cleaved mica surface and the tip of the nanotube (shown in Fig. 1). *a*, Three frequency scans were taken at the surface heights marked on the inset: A while the cantilever was oscillating freely in air, B while the nanotube at the tip of the cantilever was hitting the surface at the midpoint of the oscillation, and C while the nanotube was flexing in continuous contact with the surface throughout the oscillation. *b*, The result of a direct numerical simulation of the experiment of *a*, assuming the equation of motion of the cantilever is $Md^2z/dt^2 = F - P\sin(\omega t - \varphi)$, where frequency $F = F_{air} = k_c z + C\,dz/dt$ when the cantilever is oscillating freely in air, and $F = F_{air} + F_{EULER} + C_n\,dz/dt$ when the nanotube is in contact with the surface, P is the amplitude of the driving oscillator at frequency ω, $C = M\omega_c/Q_c$ is the viscous damping factor of the cantilever alone, $C_n = M\omega_c/Q_n$ is an additional damping term due to flexing of the nanotube, M is the effective mass of the cantilever (6×10^{-6} g), and F_{EULER} is the Euler buckling force (equation (1)). (Here ϕ is a phase shift, k_c is the cantilever force constant, and Q_c and Q_n are the quality factors of the cantilever and nanotube, respectively). The simulation plotted in *b* is for $\omega_c/2\pi = 234.8$ kHz, $k_n = 100\,N\,m^{-1}$, $Q_c = 360$, $Q_n = 3,000$, P adjusted to give a peak-to-peak amplitude in air of 44 nm, and $F_{EULER} = 10\,nN[L_0/(L_0 - (Z_s - z))]^2$, where $L_0 = 250$ nm, and Z_s is the z position of the mica surface as marked on the inset to *a*. The sharpness of the recovery of oscillation amplitude near $\omega^* = 254.2$ kHz was found to be a sensitive function of the buckling force, with the best fit to the data requiring $8\,nN < F_{EULER} < 10\,nN$, consistent with the expectation[26,27] that the Young's modulus of a MWNT be similar to that of in-plane graphite. In contrast to conventional tips which are often damaged by force and amplitude versus distance scans such as shown in the inset to *a*, the carbon nanotube tips are found to be extremely robust—even surviving repeated hard 'crashes' which bend the nanotube entirely out of the way, enabling the pyramidal silicon tip itself to press onto the surface.

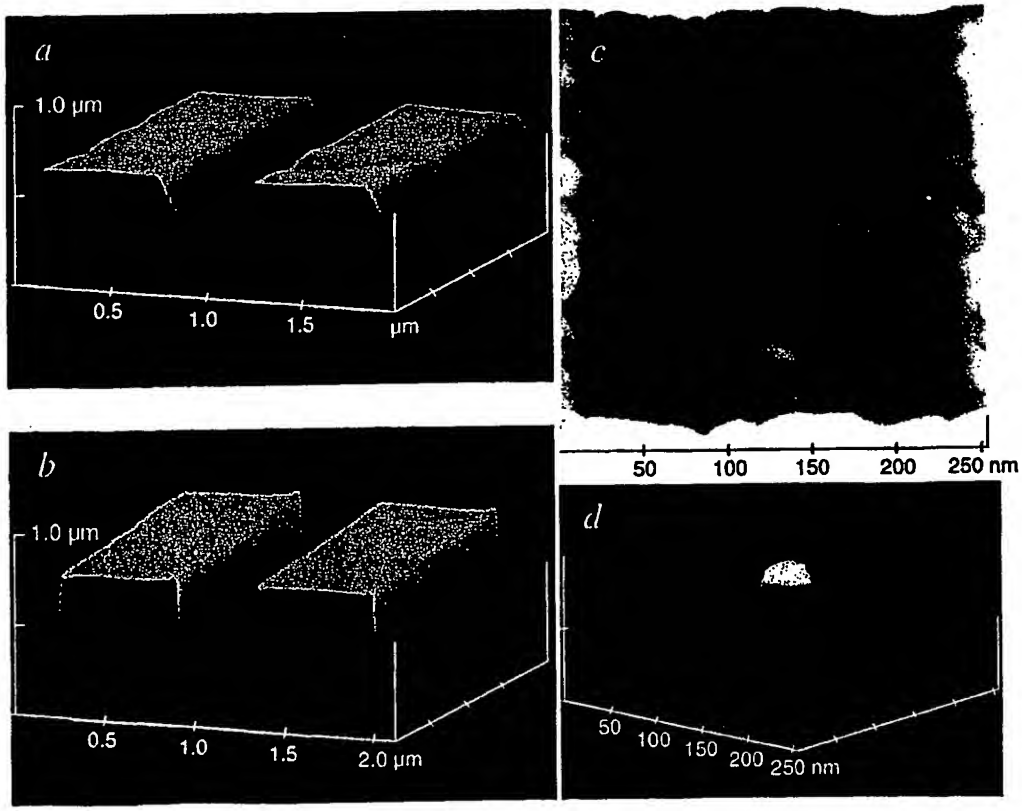

FIG. 3 Tapping-mode SFM image of a 400-nm-wide, 800-nm-deep trench etched through a TiN-coated aluminum film on a silicon wafer. *a*, Image taken with a bare pyramidal silicon tip (Digital Instruments TESP cantilever, 250 kHz resonant frequency, $100\,N\,m^{-1}$ force constant). The apparent triangular shape of the trench is an artefact due to the pyramidal shape of the imaging tip. *b*, Image taken with a nanotube attached to the pyramid of this same TESP cantilever much like that shown in Fig. 1. This thin, long nanotube is now able to reach to the bottom of the trench as shown in detail in *c* where the texture of the bottom is clearly imaged, revealing that the mean surface roughness at the bottom of the trench is ±0.4 nm. Nanotube probes provided equal or better resolution than commercial tips in all of the samples examined so far (five or six various types). *d*, Tapping-mode SFM image of a 40-nm-diameter 30-nm-high carbon dot formed on the bottom of the trench by applying a −5 V voltage pulse to the nanotube while it was held 30 nm above the bottom, after applying a 5-nm-thick gold coating to render the surface of the trench electrically conducting. Note that the axis numbers in *a* and *b* are μm, and those in *c* and *d* are nm.

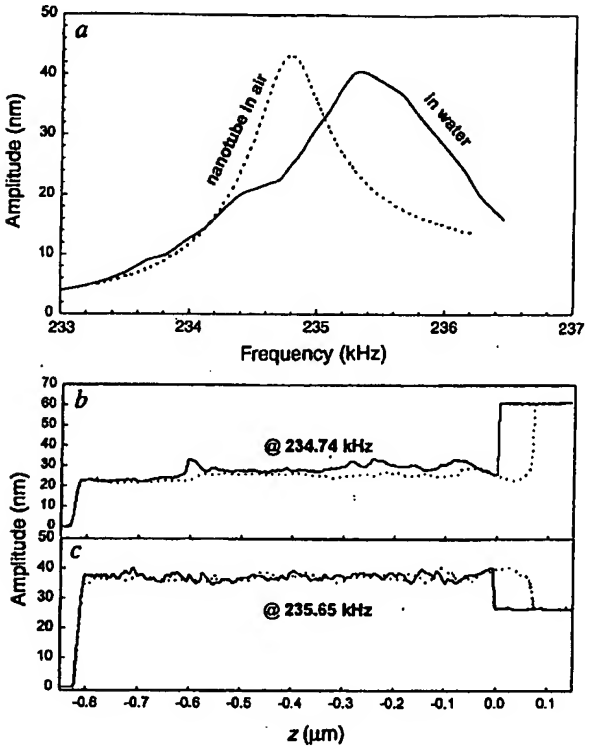

FIG. 4 *a*, Frequency response of a cantilever in air (dashed line), and with the nanotube at its tip extending 0.8 μm into a water-flooded trench similar to that shown in Fig. 3 (solid line), illustrating that such nanotube tips will permit tapping-mode experiments to be done under water even though the cantilever itself remains entirely in air. Amplitude change on dipping a nanotube probe into the flooded trench. The first contact with the water surface occurs at $z = 0$. *b*, *c*, The nanotube tip encounters the bottom of the trench at $z = -820$ nm. The trace in *b* was done at the resonant frequency of the cantilever oscillating in air (234.74 kHz); the trace in *c* was obtained at 235.65 kHz where the oscillation amplitude is seen to substantially increase when the tip of the nanotube penetrates the water surface. Although we have obtained images under these conditions, they are not yet up to the standard of those in air, for reasons we believe have to do with deficiencies in our current fluid cell. We are currently working on improving the situation, and are confident that ultimately we will obtain very high-quality images under water.

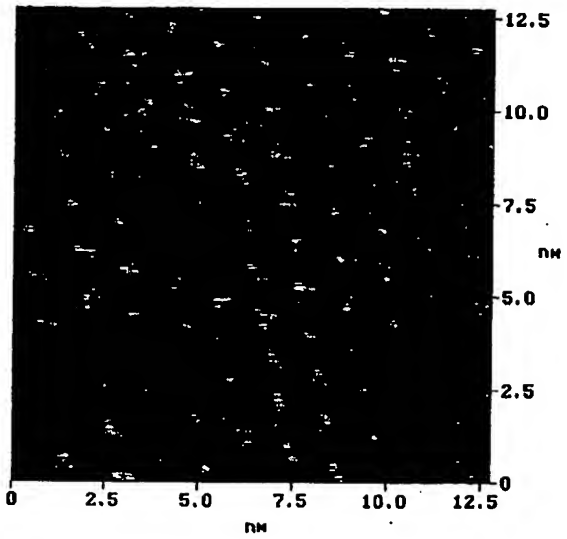

FIG. 5 Unfiltered constant-height STM image exhibiting atomic resolution and charge density waves on freshly cleaved TaS_2 surface, performed with a MWNT tip mounted similarly to that shown in Fig. 1. Bias voltage 16 mV, tunnelling current 810 pA.

length of the nanotube. Assuming the Young's modulus of the nanotube is similar to in-plane graphite (~1 TPa), the Euler bucking force of the 250-nm-long 5-nm-diameter MWBT tip shown mounted in Fig. 1 is ~5 nN. But the nanotube is also gentle because once the buckling force is exceeded the nanotube will bend easily through large amplitudes with little additional force. Euler buckling therefore serves as a kind of insurance policy during SFM imaging: the maximum force that can be transmitted to the sample is F_{EULER}. In addition, the MWNT tip is extremely gentle when touching an object laterally. The bending motion for side-directed forces is harmonic with a force constant $k_n = 3YI/L^3$. For the MWNT tip of Fig. 1, $k_n = 6.3\,\mathrm{pN\,nm^{-1}}$. When used in tapping mode, the MWNT tip shown in Fig. 1 behaves in accord with these expectations, as demonstrated in Fig. 2.

The mechanism for reduction in the tapping amplitude in operation here is almost entirely elastic. The spring force from the bending nanotube produces a coherent de-excitation of the cantilever oscillation at driving frequencies below the critical frequency ω^*. The result is that gentle, reliable SFM imaging may be accomplished in the tapping mode with even extremely stiff, high-resonant-frequency cantilevers. In contrast to the hard silicon pyramidal tip, which can easily generate impact forces >100 nN per tap if the scan is not carefully controlled[15], the MWNT probe serves as a compliant spring which moderates the impact of each tap on the surface, the peak force never exceeding F_{EULER}.

Figure 3 shows that these long, narrow MWNT tips can reach into deep trenches previously inaccessible to high-resolution scanning probes. The normal pyramidal tip is simply too wide to reach the bottom of a 0.4 μm wide 0.8 μm deep trench (Fig. 3*a*), whereas the nanotube permits the roughness of the silica surface at the bottom to be imaged easily. Also, as shown in Fig. 3*d*, it is possible using a voltage pulse on the nanotube to deposit a 40-nm dot of carbon at the bottom of the trench, and then to go back and image. Owing to the 'spring loading' of the MWNT bundle to the cantilever and the high strength and flexibility of the carbon nanotubes, SFM imaging of tortuous structures such as the trenches shown in Fig. 3 can be done without fear of damage either to the MWNT tip or the trench structure itself. In contrast, we were unable to image these trenches with an Ultralever (Park Scientific Instruments, Sunnyvale, CA) having a 4-μm-long conical silicon tip. After a few minutes of admittedly rather clumsy scanning, 80 nm of the conical tip had been broken off—a problem we expect will plague any sharp, brittle nanostructure rigidly attached at the tip of a scanning probe.

One of the principal limits in SFM imaging in air has been that at normal humidity the surface is covered with a layer of water, and the capillary adhesion forces produced when the tip makes contact are typically 10–100 nN (ref. 16). As a result, one is forced to use high-force-constant cantilevers oscillating with substantial amplitude to ensure that the tip does not get caught by the surface. Owing to the small diameter of the nanotube, we find the capillary adhesion force of MWNT tips is generally reduced to <5 nN and often as low as 0.05 nN, permitting tapping-mode imaging with cantilevers having force constants as small as $0.01\,\mathrm{N\,m^{-1}}$ at a peak-to-peak amplitude of 10 nm.

To get away entirely from the capillary adhesion force it is now conventional to image under some fluid[17]—normally water[4]. However, now that the cantilever must oscillate in water it is no longer possible to operate at high frequency and high Q (ref. 18). With a MWNT tip like the one shown in Fig. 1, it is now possible to immerse only the nanotube under the water, leaving the cantilever

Making more sense of the senses

Mind your speech. The part of the brain involved in the coordination of speech — the complex planning of mouth and tongue movements — has been identified as a region of the insula, a cortical area beneath the frontal and temporal lobes. This brain region was damaged in 25 stroke patients with 'apraxia' of speech, which is a defect in articulatory planning; but in 19 control patients with different language difficulties, this brain region was intact. Page 159.

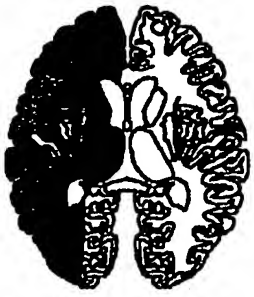

Yellow marks the brain area affected in all 25 apraxia patients.

Something in the air. Synchronized oscillations have been observed in various brain circuits, including the cerebral cortex of mammals and the brain of insects, but the function of the oscillations has been hard to determine. In the locust, odours are known to evoke oscillations in the olfactory antennal lobe neurons. Wehr and Laurent show that groups of these neurons exhibit precisely timed patterns of firing that are stimulus specific and hence likely to encode olfactory information. Pages 162 and 115.

Tracking the messenger. Many of the modulatory neurotransmitters involved in the nervous system use cyclic AMP as their second messenger. Now for the first time, cAMP indicators have been used to image the pattern of diffusion of the cAMP signal in an intact and functioning neural circuit. Pages 166 and 113.

Catch a wave — the fluorescent marker reveals cAMP on the move.

Quick thinking. A new combination of techniques makes it possible to study the timing of neurotransmission at fast synapses in the rat brain. The 'classical' view that most of the presynaptic Ca^{2+} influx occurs during the downstroke of the action potential (a model developed from the study of squid giant axons at low temperature) is found to hold only at room temperature. At physiological temperatures, synaptic delays are much shorter than in the classical model, as a result of calcium entry during the rising phase of the presynaptic action potential, which leads to extremely fast calcium-driven vesicle fusion. Page 170.

We're here because we're here

The anthropic principle, which suggests that the Universe *must* have those properties that allow life to develop in it at some stage of its life history, because if it didn't we wouldn't be here to notice it, has gained considerable popularity among cosmologists. But, in a Commentary on page 107, John Maynard Smith and Eörs Szathmáry show why, as evolutionary biologists, they have reservations. Faced with a need for historical explanation, the anthropic principle is, they argue, a cop-out.

HIV bound

Infection with HIV-1 requires the β-chemokine receptor CCR-5, and individuals lacking functional CCR-5 receptors are immune to the virus. But the primary binding site for HIV-1 is the CD4 molecule, so what is the role of CCR-5? In separate reports on pages 179 and 184, Wu *et al.* and Trkola *et al.* show that gp120 (the viral envelope protein responsible for target-cell binding) can interact directly with CCR-5, but that prior interaction with CD4 greatly increases its affinity. Neutralizing antibodies directed against either CD4-induced or V3 epitopes on gp120 block its interaction with CCR-5, suggesting that the interaction between gp120 and CD4 induces a conformational change in the former that allows it to bind CCR-5 and enter the cell. News and Views, page 117.

Guide to Authors. See Vol. 383, page 844. Also available on **http://www.america.nature.com**

SCIENTIFIC CORRESPONDENCE

BOOK REVIEWS

ARTICLES

LETTERS TO NATURE